

# Can Cobalt Be Eliminated from Lithium-Ion Batteries?

Cite This: *ACS Energy Lett.* 2022, 7, 3058–3063

Read Online

ACCESS |

Metrics & More

Article Recommendations

Following the discovery of  $\text{LiCoO}_2$  (LCO) as a cathode in the 1980s, layered oxides have enabled lithium-ion batteries (LIBs) to power portable electronic devices that sparked the digital revolution of the 21st century. Since then,  $\text{LiNi}_x\text{Mn}_y\text{Co}_z\text{O}_2$  (NMC) and  $\text{LiNi}_x\text{Co}_y\text{Al}_z\text{O}_2$  (NCA) have emerged as the leading cathodes for LIBs in electric vehicle (EV) application and have become crucial components in the fight against global warming. However, the surging demand for LIBs has led to an extremely tight supply. The EV sector has already dominated the LIB market, even though EV sales were only 2–3% of total passenger vehicle sales in 2020. EV sales are expected to grow 10-fold by the end of this decade, and close to 90% of the total LIB demand will come from the EV sector.<sup>1</sup> As a result, LIB manufacturers must aggressively ramp up cell production to keep pace with the immense growth of the EV market, a quest that brings scrutiny to the cost and sustainability of current LIB manufacturing practices. Cathodes are a critical component that largely determines the energy density and 40–50% of the total cell cost in LIBs. Rigorous consideration of the cathode performance and material cost is crucial in sustaining EV adoption. In this Viewpoint, we discuss why using cobalt in cathodes is unsustainable in the long run and highlight the features of cobalt-free cathodes.

The cost of cathodes largely depends on the cost of raw materials, such as lithium, nickel, cobalt, manganese, and iron. Among these elements, cobalt is the most problematic because of its price volatility, fragile supply chain, and human cost. Depending on the cathode composition, 80–200 g of cobalt per kWh is usually incorporated into commercial LIBs (Figure 1a).<sup>2</sup> The price of cobalt has seen dramatic swings from US\$30  $\text{kg}^{-1}$  to US\$90  $\text{kg}^{-1}$  in the past decade and has recently experienced a steeper price increase to US\$50  $\text{kg}^{-1}$  compared to that of nickel and copper (Figure 1b).<sup>3–5</sup> Such a price increase is inevitably tied to the supply chain shortages. The global production of cobalt is estimated to be only 170,000 tons, which is much less than that of nickel at 2,700,000 tons in 2021 (Figure 1c).<sup>6</sup> While increasing raw material supply can mitigate price inflation, the expansion of cobalt mining is challenging. Cobalt is primarily mined as a byproduct of nickel and copper ores since its concentration in these ores is typically 10 times lower.<sup>7</sup> Cobalt reserves and processing facilities are predominantly located in the Democratic Republic of Congo (DRC) and China, respectively (Figure 1d). Such a concentration of cobalt sourcing not only makes supply expansion difficult but also creates geopolitical risks that can

further weaken the supply chain.<sup>8</sup> Furthermore, the exploitation of child labor to mine toxic cobalt in DRC raises serious health and ethical concerns.<sup>9</sup> While LIB recycling can alleviate some of the material supply shortage, its recovery output has yet to keep up with the accelerating demand of LIBs. As such, there is a consensus within the LIB industry to reduce or abolish the use of cobalt in cathodes for cost and sustainability reasons.

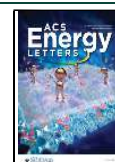
Cobalt has long been an essential element within the layered oxide family of cathodes, ranging from the parent composition LCO to the NMC family with varying Ni/Mn/Co ratios. LCO maintains its dominance in the portable electronic market because of its superior cycling stability, volumetric capacity, and ease of synthesis, yet it is far too expensive for EV applications. Additionally, the overlap of the  $\text{Co}^{3+/4+}t_{2g}$  band with the top of the  $\text{O}^{2-}2p$  band in LCO limits full Li extraction and its usable specific capacity (Figure 2).<sup>10</sup> Substituting Co with Ni and Mn is a viable route to increase usable specific capacity by utilizing  $\text{Ni}^{2+/3+}$  and  $\text{Ni}^{3+/4+}$  redox centers while keeping the advantages of Co, such as good electronic conduction and low Li/Ni mixing for facile ionic conduction. Hence, layered oxides with increasing Ni content have been slowly adopted, progressing from  $\text{LiNi}_{0.33}\text{Mn}_{0.33}\text{Co}_{0.33}\text{O}_2$  (NMC-333) to  $\text{LiNi}_{0.8}\text{Mn}_{0.1}\text{Co}_{0.1}\text{O}_2$  (NMC-811). At the limit of Ni content is the archetypical high-energy material  $\text{LiNiO}_2$  (LNO), which delivers an average voltage of  $\sim 3.8 V_{\text{Li}}$  (V vs  $\text{Li}/\text{Li}^+$ ) and a specific capacity of up to  $\sim 240\text{--}250 \text{ mA h g}^{-1}$ .

However, increasing the Ni content in layered oxides also increases surface, structural, and thermal instabilities that adversely affect battery lifetime and safety. With a fuller degree of lithium extraction at a high state-of-charge (SoC), high-Ni layered oxides experience a phase transformation ( $\text{H}_2 \rightarrow \text{H}_3$ ) that causes a large anisotropic contraction and the collapse of the layered structure (Figure 2b).<sup>11</sup> The structural strain induces inter- and intragranular cracking, loss of interparticle contact, and loss of active materials through defect and rock-salt formation.  $\text{Ni}^{3+/4+}$  species also react aggressively with the

Received: July 7, 2022

Accepted: August 9, 2022

Published: August 22, 2022



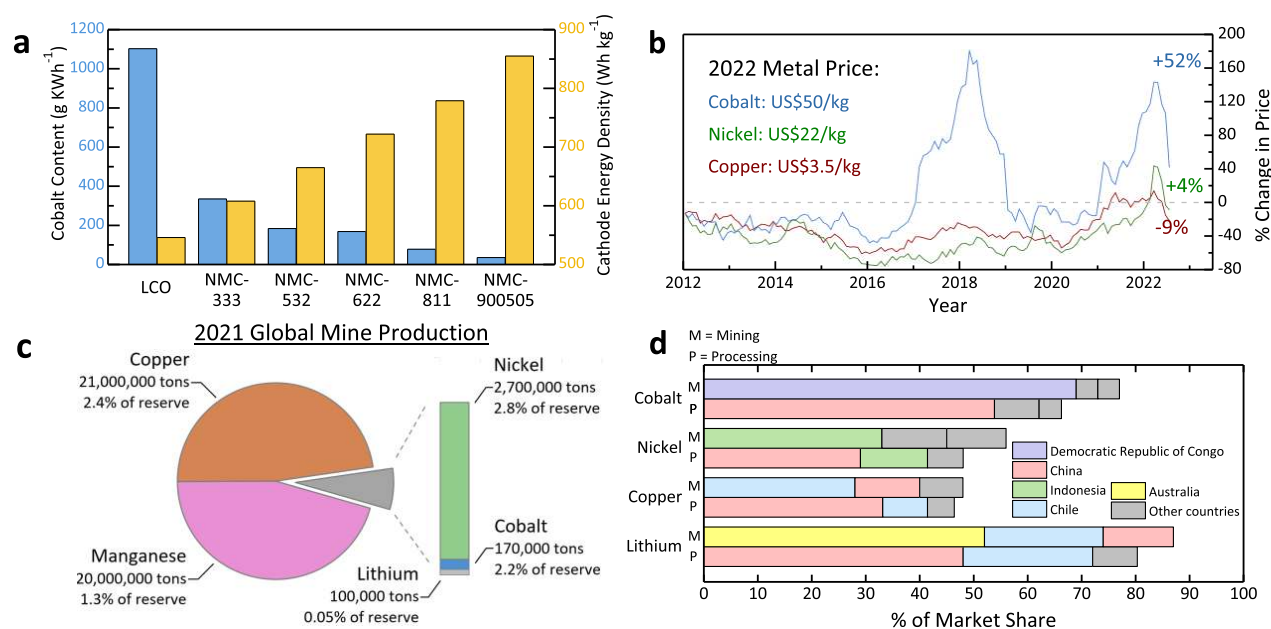


**Figure 1.** (a) Energy density and cobalt content of typical layered oxides, ranging from LiCoO<sub>2</sub> (LCO) to LiNi<sub>x</sub>Mn<sub>y</sub>Co<sub>z</sub>O<sub>2</sub> (NMC-xyz) of increasing nickel content. (b) Price chart of raw cobalt, nickel, and copper in the past decade (2012 to August 2022).<sup>3–5</sup> (c) Global mine production of nickel, cobalt, lithium, copper, and manganese in 2021.<sup>6</sup> (d) Supply chain breakdown of cobalt, nickel, copper, and lithium mining and processing by countries.<sup>8</sup>

electrolyte, resulting in surface spinel-like and rock-salt phase formation, consumption of active Li inventory, and cell impedance growth. During thermal runaway, high-Ni layered oxides experience a larger exothermic energy release at a lower onset temperature, which jeopardizes battery safety.<sup>12</sup> Nevertheless, rational compositional designs and materials engineering strategies on high-Ni layered oxides, such as surface coatings and electrolyte modifications, have seen some success in alleviating these instability issues. Hence, high-Ni layered oxide cathodes remain an ideal choice for EV applications due to their high energy density, sufficient cycle life and rate performance, and long-established large-scale synthesis infrastructure.

The question remains whether Co is necessary for sufficient electrochemical performance of high-Ni layered oxide cathodes. The prevailing belief is that Co<sup>3+</sup> is essential for charge balancing to alleviate the negative effect of Mn<sup>4+</sup> in inducing Ni<sup>2+</sup> formation. Ni<sup>2+</sup> tends to occupy the Li<sup>+</sup> site (Li/Ni mixing), which blocks lithium diffusion pathways and slows the charge/discharge kinetics. This leads to efforts in replacing Mn<sup>4+</sup> with Al<sup>3+</sup>, which offers some of the same benefits as Co<sup>3+</sup> in reducing Li/Ni mixing, enhancing charge/discharge rate capability, improving thermal stability, and lowering surface reactivity. As a result, LiNi<sub>0.8</sub>Co<sub>0.15</sub>Al<sub>0.05</sub>O<sub>2</sub> (NCA-80) has an improved cycling stability compared to that of LiNi<sub>0.8</sub>Co<sub>0.2</sub>O<sub>2</sub> (NC-8020) and LiNi<sub>0.7</sub>Mn<sub>0.15</sub>Co<sub>0.15</sub>O<sub>2</sub> (NMC-701515). However, this is likely not caused by Mn removal but instead by the benefit of Al in suppressing parasitic surface reactions at high SoC.<sup>13–15</sup> In fact, contrary to popular belief, a small amount of Ni<sup>2+</sup> in the Li<sup>+</sup> layer induced by Mn<sup>4+</sup> may actually be beneficial in providing structural stabilization as a pillaring ion.<sup>16</sup> Similarly, Mg<sup>2+</sup> is also effective at stabilizing high-Ni cathodes at high SoC by residing in the Li<sup>+</sup> site as a pillaring ion.<sup>17</sup> On the other hand, Co<sup>3+</sup> does not seem to impart any electrochemical, structural, and thermal stability benefit compared to Mn<sup>4+</sup>, Al<sup>3+</sup>, and Mg<sup>2+</sup> up to 10% doping in

LNO.<sup>18</sup> While Co<sup>3+</sup> may be useful for NMC with high Mn<sup>4+</sup> content, these observations suggest that Co<sup>3+</sup> is not necessary for high-Ni layered oxide cathodes. Alternative dopants like Mn<sup>4+</sup>, Al<sup>3+</sup>, and Mg<sup>2+</sup> can provide sufficient structural and surface stabilization benefits that enable high-Ni layered oxides with high energy density and electrochemical stability.

Our recent research has revealed the benefit of the Mn–Al combination in promoting a high-Ni, cobalt-free cathode (LiNi<sub>0.9</sub>Mn<sub>0.05</sub>Al<sub>0.05</sub>O<sub>2</sub>, NMA-900505) with promising electrochemical performance compared to that of its cobalt-containing peer with the same Ni content (~90%). We have demonstrated the importance of Al<sup>3+</sup> in mitigating Li/Ni mixing and enhancing cycling stability, rate capability, and thermal stability of NMA-900505.<sup>19</sup> Post mortem analysis further confirms that Al<sup>3+</sup> doping is crucial to the electrochemical stability of high-Ni cathodes, and Co<sup>3+</sup> is not necessary when Al<sup>3+</sup> is present. Even a small amount of Al<sup>3+</sup> and Mg<sup>2+</sup> doping in LiNi<sub>0.9</sub>Mn<sub>0.04</sub>Co<sub>0.04</sub>Al<sub>0.01</sub>Mg<sub>0.01</sub>O<sub>2</sub> (NMCAM-9004040101) dramatically improves the cyclability of NMC-900505 by reducing surface reactivity and particle pulverization.<sup>20</sup> This proves the potential of Mn–Al and Mn–Al–Mg combinations in yielding a wide range of high-Ni, cobalt-free cathodes with high energy density and durability.<sup>16,21</sup> Aside from these elements, titanium can further improve high-Ni cathodes by creating a protective surface coating that mitigates parasitic side reactions with the electrolyte. We demonstrated the combined benefits of Al<sup>3+</sup>, Mg<sup>2+</sup>, and Ti<sup>3+</sup> in promoting robust cycling stability in LiNi<sub>0.93</sub>Al<sub>0.05</sub>Ti<sub>0.03</sub>Mg<sub>0.01</sub>O<sub>2</sub> (NATM) compared to NMC-900505, illustrating again the promise of eliminating Co in next generation high-Ni cathodes for EV applications.<sup>22</sup> Without being subjected to the material availability and high price of Co, these cobalt-free cathode compositions will likely gain immense traction in the EV battery market as promising low-cost alternatives. However, air storage instability and scalability of calcination with oxygen flow need to be addressed

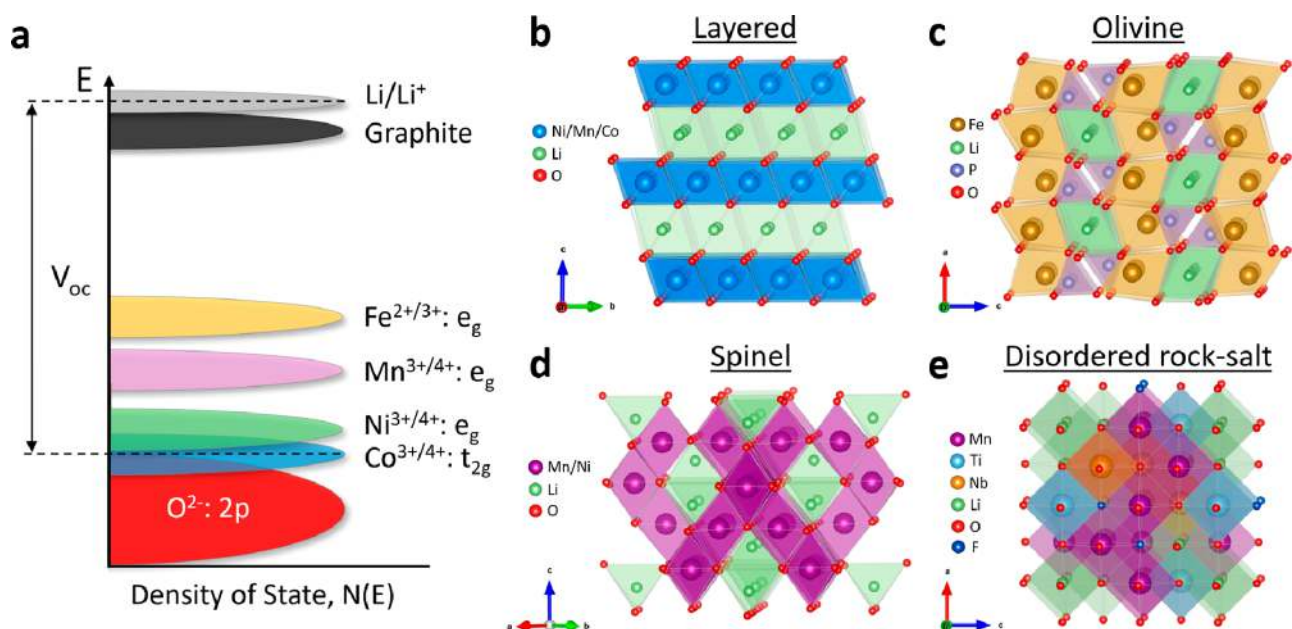


**Figure 2.** (a) Redox energies of cobalt (Co), nickel (Ni), manganese (Mn), and iron (Fe) relative to those of lithium (Li) and graphite. Crystal structures of (b) layered oxide  $\text{LiNi}_x\text{Mn}_y\text{Co}_z\text{O}_2$ , (c) olivine  $\text{LiFePO}_4$ , (d) spinel  $\text{LiNi}_x\text{Mn}_y\text{O}_4$ , and (e) disordered rock-salt  $\text{Li}_2\text{Mn}_w\text{Nb}_x\text{Ti}_y\text{O}_{3-z}\text{F}_z$ .

for high-Ni cathodes to achieve the same production scale as lower-Ni cathodes (Ni content  $\leq 70\%$ ).

In theory, many other 3d transition metals are capable of electrochemical redox activity besides Co and Ni. Selection criteria, such as redox energy (Figure 2), phase stability, voltage profile continuity, material abundance, and toxicity dictate the feasibility of cathode chemistries for commercial use. Although lower in energy density, Fe- and Mn-based cathodes are attractive alternatives to Co- and Ni-based cathodes for EV applications due to the abundance of raw material. Feasible Fe-based cathodes mainly exist in poly-anionic forms ( $\text{BO}_3^{-2}$ ,  $\text{SiO}_4^{-4}$ ,  $\text{PO}_4^{-3}$ ,  $\text{SO}_4^{-2}$ ,  $\text{P}_2\text{O}_7^{-4}$ , etc.), as the electronic configuration of  $\text{Fe}^{2+/3+}$  does not encourage a layered  $\text{LiFeO}_2$  structure with reversible lithium insertion ability.<sup>10</sup> Considering the inductive effect, which dictates the  $\text{Fe}^{2+/3+}$  redox energy, and the access to compositions with necessary structural features,  $\text{LiFePO}_4$  (LFP) is the most ideal Fe-based composition that delivers decent material-level energy density ( $\sim 3.4 \text{ V}_{\text{Li}}$ ,  $\sim 160 \text{ mA h g}^{-1}$ ).<sup>23,24</sup> The olivine structure of LFP has a rigid network of covalent P–O–Fe bonds with rapid one-dimensional Li diffusion channels (Figure 2c). Combined with the facile phase transformation kinetics with nanosized particles and low cutoff charge voltage ( $\sim 3.6 \text{ V}$ ), LFP exhibits an exceptional cycle life and rate capability as well as robust tolerance to extreme operating conditions. However, LFP is a poor electronic conductor and requires surface carbon coating to promote sufficient electronic percolation throughout the electrode. A careful control of synthesis conditions is necessary to produce LFP with a uniform carbon coating, high phase purity, and low antisite defects.<sup>25</sup> The electrode thickness of LFP is much higher than that of layered oxides to compensate for its low volumetric capacity and enable practical cell-level energy density. As such, at high cathode areal loadings ( $>3 \text{ mA h cm}^{-2}$ ), diffusion limitations in the electrolyte markedly limit the usable energy and power of LFP-based LIBs, especially at low temperatures.<sup>26</sup> Although Mn-substituted  $\text{LiMn}_x\text{Fe}_y\text{PO}_4$  can theoret-

ically increase the average working voltage ( $\text{Mn}^{2+/3+}$  redox at  $\sim 4.1 \text{ V}_{\text{Li}}$ ), the large voltage difference ( $\sim 0.7 \text{ V}$ ) between the  $\text{Fe}^{2+/3+}$  and  $\text{Mn}^{2+/3+}$  redox reactions in LMFP creates a sudden voltage drop during battery use, which is not ideal for power electronics. For  $\text{LiMnPO}_4$  (LMP), anisotropic strain caused by Jahn–Teller active  $\text{Mn}^{3+}$  ions hinders the charge/discharge kinetics and limits its practical applications.<sup>27</sup> Despite the lower energy density of LFP, EV battery manufacturers are ramping up the use of LFP because of its abundant and low-cost raw materials. Battery pack engineers leverage the excellent thermal stability of LFP to eliminate the use of thermal management systems that contribute to the inactive mass of the battery pack. New generations of EV battery packs can integrate high-capacity prismatic LFP cells into a novel structural battery pack architecture without using battery modules.<sup>28</sup> The cell-to-pack packing efficiency of LFP-based battery packs is 40% higher than that of Ni-based layered oxide battery packs, thus enabling a cost-effective battery pack with competitive energy density.<sup>29</sup> Such an engineering breakthrough marks a critical turning point for LFP and enables the mass adoption of LFP-based LIBs into low-cost EVs. However, production of LFP-based LIBs should be diversified outside of China to ensure a robust supply chain for global EV manufacturers.

Contrary to Fe-based cathodes, Mn-based cathodes exhibit a wide range of possible chemical compositions and crystal structures. The unique electronic configuration of  $\text{Mn}^{2+/3+/4+}$  enables its oxides to take form in a layered (Figure 2b), spinel (Figure 2d), or a rock-salt structure (Figure 2e) with vastly different electrochemical characteristics.<sup>30</sup> However, Mn-based cathodes generally suffer from poor electrochemical stabilities due to Mn dissolution,<sup>31,32</sup> cation ordering,<sup>33,34</sup> and surface reconstruction problems that are often interconnected.<sup>35</sup> The layered  $\text{LiMnO}_2$  phase exhibits a sloping voltage profile at  $\sim 3 \text{ V}$  and provides  $\sim 200 \text{ mA h g}^{-1}$  of specific capacity, while the spinel  $\text{LiMn}_2\text{O}_4$  (LMO) phase exhibits a flat voltage profile at  $\sim 4 \text{ V}$  and provides only  $\sim 110 \text{ mA h g}^{-1}$  of specific capacity.

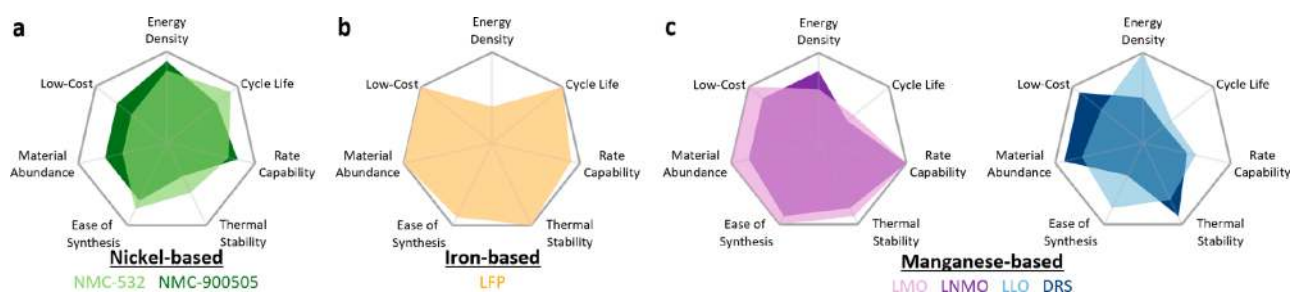


**Figure 3.** Performance comparison of (a) nickel-based, (b) iron-based, and (c) manganese-based cathodes. Energy density is based on the material level by multiplying average voltage with specific capacity. Cycle life is determined by the lifetime of full cells that are paired with a graphite anode. Rate capability is based on the materials' properties, such as ionic/electronic conductivity and phase transformation kinetics. Thermal stability is based on the peak temperature of thermal runaway and amount of heat flow. Ease of synthesis is determined by material synthesis conditions (precursor selection, reaction environment, carbon coating, high-energy ball-milling, etc.). Material abundance and low cost are determined by the elemental abundance on the earth's crust and the price of raw materials, respectively.

Although  $\text{LiMnO}_2$  is more energy dense, the layered structure is unstable as it readily transforms into a spinel structure during cycling, even if the initial material contains a stoichiometric Li to Mn ratio.<sup>30,36</sup> In contrast, LMO retains the spinel structure over the course of cycling and thus has been employed in some commercial EVs in the past. A three-dimensional network of edge-sharing  $\text{MnO}_6$  octahedra in the spinel framework and the direct communication between mixed-valent  $\text{Mn}^{3+/4+}$  atoms enable fast rate capability in LMO (Figure 2d). The more ionic nature of the Mn–O bond also renders Mn-based cathodes thermally more stable than Co- and Ni-based cathodes. Substituting 25% of  $\text{Mn}^{4+}$  with  $\text{Ni}^{2+}$  enables  $\text{LiNi}_{0.5}\text{Mn}_{1.5}\text{O}_4$  (LNMO) with a high an operating voltage of  $\sim 4.7 V_{\text{Li}}$  and a specific capacity of  $\sim 135 \text{ mA h g}^{-1}$  by utilizing a  $\text{Ni}^{2+/3+}$  redox center instead of a  $\text{Mn}^{3+/4+}$  redox. This high-voltage spinel retains the structural stability, fast ionic/electronic transport properties, and most of the cost advantage of LMO, making this cathode composition attractive for high-energy and high-power applications. The main deterrent for LNMO is the lack of a high-voltage electrolyte formulation that supports a stable cathode–electrolyte interface.

Increasing the Li/Mn stoichiometry in the Li–Mn–O system leads to rock-salt  $\text{Li}_2\text{MnO}_3$  or layered  $\text{Li}[\text{Li}_{1/3}\text{Mn}_{2/3}]\text{O}_2$ , where one-third of the  $\text{Li}^+$  ions reside in the transition metal plane (Figure 2b). While  $\text{Mn}^{4+}$  cannot be oxidized further upon lithium extraction, it was later found that lithium extraction is achievable when the anionic redox of  $\text{O}^{2-}$ :2p band is activated at 4.5 V, delivering  $\sim 250 \text{ mA h g}^{-1}$  at  $\sim 3 V_{\text{Li}}$ .<sup>37</sup> Anionic redox generally leads to excess oxygen release, but it can be somewhat mitigated by incorporating nanodomains of  $\text{Li}_2\text{MnO}_3$  into traditional layered oxides (e.g., NMC-333 or  $\text{LiNi}_{0.5}\text{Mn}_{0.5}\text{O}_2$ ). This gives rise to  $x\text{Li}_2\text{MnO}_3 \cdot (1-x)\text{LiMO}_2$  ( $M = \text{Ni, Co, Mn, etc.}$ ) or Li-rich layered oxides (LLO). LLO provides a high specific capacity of  $\sim 250\text{--}300 \text{ mA h g}^{-1}$  at  $\sim 3.6 V_{\text{Li}}$  with only a small fraction of Ni and Co.<sup>38</sup> Such a benefit is largely negated by the same instability issues of  $\text{LiMn}_2\text{O}_3$  that induce voltage decay, substantial electrolyte oxidation reactions, and an overall performance deterioration much faster than that of traditional Li stoichiometric layered oxides.<sup>12</sup>

A new strategy to stabilize the  $\text{Li}_2\text{MnO}_3$  structure has led to a new class of cathodes and expanded the compositional range of Mn-based oxide cathodes. Disordered rock-salt (DRS) materials ( $\text{Li}_2\text{Mn}_{1-x}\text{M}_x\text{O}_{3-y}\text{F}_y$ ,  $M = \text{Ti, Nb, Mo, etc.}$ ) can leverage both  $\text{Mn}^{2+/3+}$  and  $\text{Mn}^{3+/4+}$  redox centers to generate a high specific capacity of  $\sim 300 \text{ mA h g}^{-1}$  at an average voltage

of  $\sim 3 V_{\text{Li}}$  when cycled from 1.5 to 5.0  $V_{\text{Li}}$ .<sup>39</sup> Activating the electrochemistry and stabilizing the structure of  $\text{Li}_2\text{MnO}_3$  requires careful material engineering to ensure percolating diffusion pathways for Li mobility (i) using excess Li, (ii) inducing a cation-disordered structure (Figure 2e), (iii) substituting Mn with high-valent cations ( $\text{Ti}^{4+}$ ,  $\text{Nb}^{5+}$ ,  $\text{Mo}^{6+}$ , etc.) and oxygen with fluorine, and (iv) reducing the particle size into a submicron regime via ball-milling.<sup>40</sup> Because of its relatively short research history, comprehensive understanding of the interplay between chemical composition, synthesis condition, structural property, and electrochemical performance of DRS remains to be further explored and understood. In addition, several critical hurdles must be overcome for this class of material to achieve practical relevance. For instance, nanosized particles exacerbate surface reactivity (e.g., Mn dissolution) and reduce its tap density and energy density. Oxygen release can still occur at high potential even if substantial fluorine (>10%) is incorporated, and large amounts of fluorine can only be incorporated with high-energy ball-milling, which may pose challenges for industrial scalability. Lastly, composite electrodes made with DRS typically use excess amounts of conductive carbon (10–20%), which further decreases its energy density. In short, while Mn-based oxide cathodes are cheap, abundant, and environmentally friendly, fundamental issues associated with them may pose challenges for EV applications in the near term unless issues with Mn dissolution, irreversible structural changes, oxygen release, and cathode–electrolyte interfacial instabilities are addressed.

With many potential cobalt-free cathodes for LIBs, the selection criteria will narrow down to the performance need of a particular application in terms of energy density, cycle life, rate capability, thermal stability, synthesis process, material availability, and cost (Figure 3). For most EVs and electric aviation, layered oxides will remain the dominant force for the foreseeable future. For EVs with more cost sensitivity and less range requirement, LFP is a viable option given that the pack-level energy density is adequate. The advent of solid-state battery technologies could potentially enable Mn-based cathodes by inhibiting Mn dissolution and crossover to the anode. Research efforts on future metal-free cathode chemistries like sulfur and alternative working ions, such as sodium and multivalent ions, may pave the way to enabling low-cost energy storage solutions for large-scale grid storage. These new chemistries will diversify the battery landscape and help alleviate the overconcentration of cobalt- and soon nickel-

based LIBs to sustain the expansion of electric transportation and renewable energy technologies broadly.

Steven Lee, Graduate Student

Arumugam Manthiram  [orcid.org/0000-0003-0237-9563](https://orcid.org/0000-0003-0237-9563)

## AUTHOR INFORMATION

Complete contact information is available at:

<https://pubs.acs.org/10.1021/acseenergylett.2c01553>

## Notes

The authors declare the following competing financial interest(s): The corresponding author (A.M.) is a co-founder of TexPower EV Technologies, a start-up company focusing on cobalt-free cathode materials for lithium-based batteries.

## ACKNOWLEDGMENTS

The authors acknowledge the support from the Assistant Secretary for Energy Efficiency and Renewable Energy, Office of Vehicle Technologies of the U.S. Department of Energy Award Number DE-EE0008445 and Welch Foundation Grant F-1254. Views expressed in this Viewpoint are those of the authors and not necessarily the views of the ACS.

## REFERENCES

- (1) Woodward, M.; Walton, B.; Hamilton, J.; Alberts, G.; Fullerton-Smith, S.; Day, E.; Ringrow, J. *Electric Vehicles - Setting a Course for 2030*; Deloitte Insights; <https://www2.deloitte.com/us/en/insights/focus/future-of-mobility/electric-vehicle-trends-2030.html> (accessed 2022-02-09).
- (2) Li, W.; Erickson, E. M.; Manthiram, A. High-Nickel Layered Oxide Cathodes for Lithium-Based Automotive Batteries. *Nature Energy* **2020**, *5*, 26–34.
- (3) *Cobalt Futures (CBDc1)*; <https://www.investing.com/commodities/cobalt> (accessed 2022-07-29).
- (4) *Nickel Futures (MNKc1)*; <https://www.investing.com/commodities/nickel> (accessed 2022-07-29).
- (5) *Copper Futures (HGK2)*; <https://www.investing.com/commodities/copper> (accessed 2022-07-29).
- (6) U.S. Geological Survey. *Mineral Commodity Summaries 2022*, DOI: 10.3133/mcs2022.
- (7) Olivetti, E. A.; Ceder, G.; Gaustad, G. G.; Fu, X. Lithium-Ion Battery Supply Chain Considerations: Analysis of Potential Bottlenecks in Critical Metals. *Joule* **2017**, *1*, 229–243.
- (8) IEA. *The Role of Critical World Energy Outlook Special Report Minerals in Clean Energy Transitions*; <https://www.iea.org/reports/the-role-of-critical-minerals-in-clean-energy-transitions> (accessed 2022-07-31).
- (9) Frankel, T. C. *The Cobalt Pipeline*; The Washington Post; <https://www.washingtonpost.com/graphics/business/batteries/congo-cobalt-mining-for-lithium-ion-battery/> (accessed 2022-07-31).
- (10) Manthiram, A. A Reflection on Lithium-Ion Battery Cathode Chemistry. *Nat. Commun.* **2020**, *11*, 1550.
- (11) Li, W.; Asl, H. Y.; Xie, Q.; Manthiram, A. Collapse of  $\text{LiNi}_{1-x-y}\text{Co}_x\text{Mn}_y\text{O}_2$  Lattice at Deep Charge Irrespective of Nickel Content in Lithium-Ion Batteries. *J. Am. Chem. Soc.* **2019**, *141* (13), 5097–5101.
- (12) Li, W.; Song, B.; Manthiram, A. High-Voltage Positive Electrode Materials for Lithium-Ion Batteries. *Chem. Soc. Rev.* **2017**, *46*, 3006–3059.
- (13) Zhou, K.; Xie, Q.; Li, B.; Manthiram, A. An In-Depth Understanding of the Effect of Aluminum Doping in High-Nickel Cathodes for Lithium-Ion Batteries. *Energy Storage Materials* **2021**, *34* (September 2020), 229–240.
- (14) Li, J.; Li, W.; Wang, S.; Jarvis, K.; Yang, J.; Manthiram, A. Facilitating the Operation of Lithium-Ion Cells with High-Nickel Layered Oxide Cathodes with a Small Dose of Aluminum. *Chem. Mater.* **2018**, *30*, 3101–3109.
- (15) Li, W.; Liu, X.; Celio, H.; Smith, P.; Dolocan, A.; Chi, M.; Manthiram, A. Mn versus Al in Layered Oxide Cathodes in Lithium-Ion Batteries: A Comprehensive Evaluation on Long-Term Cyclability. *Adv. Energy Mater.* **2018**, *8*, 1703154.
- (16) Liu, T.; Yu, L.; Liu, J.; Lu, J.; Bi, X.; Dai, A.; Li, M.; Li, M.; Hu, Z.; Ma, L.; Luo, D.; Zheng, J.; Wu, T.; Ren, Y.; Wen, J.; Pan, F.; Amine, K. Understanding Co Roles towards Developing Co-Free Ni-Rich Cathodes for Rechargeable Batteries. *Nature Energy* **2021**, *6*, 277–286.
- (17) Xie, Q.; Li, W.; Manthiram, A. A Mg-Doped High-Nickel Layered Oxide Cathode Enabling Safer, High-Energy-Density Li-Ion Batteries. *Chem. Mater.* **2019**, *31* (3), 938–946.
- (18) Li, H.; Cormier, M.; Zhang, N.; Inglis, J.; Li, J.; Dahn, J. R. Is Cobalt Needed in Ni-Rich Positive Electrode Materials for Lithium Ion Batteries? *J. Electrochem. Soc.* **2019**, *166* (4), A429–A439.
- (19) Li, W.; Lee, S.; Manthiram, A. High-Nickel NMA: A Cobalt-Free Alternative to NMC and NCA Cathodes for Lithium-Ion Batteries. *Adv. Mater.* **2020**, *32* (33), 2022718.
- (20) Lee, S.; Li, W.; Dolocan, A.; Celio, H.; Park, H.; Warner, J. H.; Manthiram, A. In-Depth Analysis of the Degradation Mechanisms of High-Nickel, Low/No-Cobalt Layered Oxide Cathodes for Lithium-Ion Batteries. *Adv. Energy Mater.* **2021**, *11* (31), 2100858.
- (21) Yi, M.; Li, W.; Manthiram, A. Delineating the Roles of Mn, Al, and Co by Comparing Three Layered Oxide Cathodes with the Same Nickel Content of 70% for Lithium-Ion Batteries. *Chem. Mater.* **2022**, *34*, 629.
- (22) Cui, Z.; Xie, Q.; Manthiram, A. A Cobalt- and Manganese-Free High-Nickel Layered Oxide Cathode for Long-Life, Safer Lithium-Ion Batteries. *Adv. Energy Mater.* **2021**, *11* (41), 2102421.
- (23) Manthiram, A.; Goodenough, J. B. Lithium-Based Polyanion Oxide Cathodes. *Nature Energy* **2021**, *6* (8), 844–845.
- (24) Padhi, A. K.; Nanjundaswamy, K. S.; Goodenough, J. B. Phospho-Olivines as Positive Electrode Materials for Rechargeable Lithium Batteries. *J. Electrochem. Soc.* **1997**, *144* (4), 1188.
- (25) Zaghbi, K.; Mauger, A.; Julien, C. M. Overview of Olivines in Lithium Batteries for Green Transportation and Energy Storage. *J. Solid State Electrochem.* **2012**, *16* (3), 835–845.
- (26) Wang, F.; Tang, M. Thermodynamic Origin of Reaction Non-Uniformity in Battery Porous Electrodes and Its Mitigation. *J. Electrochem. Soc.* **2020**, *167* (12), 120543.
- (27) Kang, B.; Ceder, G. Electrochemical Performance of  $\text{LiMnPO}_4$  Synthesized with Off-Stoichiometry. *J. Electrochem. Soc.* **2010**, *157* (7), A808.
- (28) BYD's New Blade Battery Set to Redefine EV Safety Standards; BYD USA; <https://en.byd.com/news/byds-new-blade-battery-set-to-define-ev-safety-standards> (accessed 2022-08-02).
- (29) Yang, X. G.; Liu, T.; Wang, C. Y. Thermally Modulated Lithium Iron Phosphate Batteries for Mass-Market Electric Vehicles. *Nature Energy* **2021**, *6* (2), 176–185.
- (30) Gummow, R. J.; de Kock, A.; Thackeray, M. M. Improved Capacity Retention in Rechargeable 4 V Lithium/Lithium-Manganese Oxide (Spinel) Cells. *Ionics (Kiel)* **1994**, *69*, 59–67.
- (31) Asl, H. Y.; Manthiram, A. Reining in Dissolved Transition-Metal Ions. *Science* **2020**, *369* (6500), 140–141.
- (32) Choi, W.; Manthiram, A. Comparison of Metal Ion Dissolutions from Lithium Ion Battery Cathodes. *J. Electrochem. Soc.* **2006**, *153* (9), A1760.
- (33) Manthiram, A.; Chemelewski, K.; Lee, E. S. A Perspective on the High-Voltage  $\text{LiMn}_{1.5}\text{Ni}_{0.5}\text{O}_4$  Spinel Cathode for Lithium-Ion Batteries. *Energy Environ. Sci.* **2014**, *7* (4), 1339–1350.
- (34) Lee, E. S.; Nam, K. W.; Hu, E.; Manthiram, A. Influence of Cation Ordering and Lattice Distortion on the Charge-Discharge Behavior of  $\text{LiMn}_{1.5}\text{Ni}_{0.5}\text{O}_4$  Spinel between 5.0 and 2.0 V. *Chem. Mater.* **2012**, *24* (18), 3610–3620.
- (35) Amos, C. D.; Roldan, M. A.; Varela, M.; Goodenough, J. B.; Ferreira, P. J. Revealing the Reconstructed Surface of  $\text{Li}[\text{Mn}_2]\text{O}_4$ . *Nano Lett.* **2016**, *16* (5), 2899–2906.

(36) Armstrong, A. R.; Bruce, P. G. Synthesis of Layered  $\text{LiMnO}_2$  as Electrode for Rechargeable Lithium Batteries. *Nature* **1996**, *381*, 499–500.

(37) Yu, D. Y. W.; Yanagida, K.; Kato, Y.; Nakamura, H. Electrochemical Activities in  $\text{Li}_2\text{MnO}_3$ . *J. Electrochem. Soc.* **2009**, *156* (6), A417.

(38) Thackeray, M. M.; Kang, S. H.; Johnson, C. S.; Vaughey, J. T.; Benedek, R.; Hackney, S. A.  $\text{Li}_2\text{MnO}_3$ -Stabilized  $\text{LiMO}_2$  (M = Mn, Ni, Co) Electrodes for Lithium-Ion Batteries. *J. Mater. Chem.* **2007**, *17* (30), 3112–3125.

(39) Lee, J.; Kitchaev, D. A.; Kwon, D. H.; Lee, C. W.; Papp, J. K.; Liu, Y. S.; Lun, Z.; Clément, R. J.; Shi, T.; McCloskey, B. D.; Guo, J.; Balasubramanian, M.; Ceder, G. Reversible  $\text{Mn}^{2+}/\text{Mn}^{4+}$  Double Redox in Lithium-Excess Cathode Materials. *Nature* **2018**, *556* (7700), 185–190.

(40) Clément, R. J.; Lun, Z.; Ceder, G. Cation-Disordered Rocksalt Transition Metal Oxides and Oxyfluorides for High Energy Lithium-Ion Cathodes. *Energy Environ. Sci.* **2020**, *13* (2), 345–373.